

Electronic structure of nitrogen-carbon alloys ($a\text{-CN}_x$) determined by photoelectron spectroscopy

S. Souto, M. Pickholz, M. C. dos Santos, and F. Alvarez

Instituto de Física "Gleb Wataghin," Universidade Estadual de Campinas, Unicamp, 13083-970, Campinas, São Paulo, Brazil

(Received 27 August 1997; revised manuscript received 23 September 1997)

The electronic structure of nitrogen-containing diamondlike films prepared by sputtering was determined by photoelectron spectroscopy. The N $1s$ core-level spectra are constituted by two peaks at 400.5 and 398.2 eV associated with substitutional N sp^2 in aromatic rings and N bonded to C sp^3 , respectively. On increasing N, the top of the valence band suffers profound changes. The new features are identified by a comparison of the experimental spectra with theoretically calculated density of states of nitrogen-containing graphite and C_3N_4 structures. [S0163-1829(98)04004-1]

I. INTRODUCTION

In the last decade, amorphous carbon ($a\text{-C}$) and hydrogenated amorphous carbon ($a\text{-C:H}$) films were intensively studied because of their useful properties such as hardness, conductivity, and optical band gap. All these properties depend strongly on the preparation methods and parameter deposition. The most common are plasma-enhanced chemical-vapor deposition, sputtering (SP), and ionic bombardment.¹ Recently, nitrogen-containing amorphous carbons received particular attention for their mechanical and electro-optical properties.^{2,3} However, the main interest in C-N alloys stems from theoretical predictions of a metastable silicon-nitride-like phase, i.e., $\beta\text{-C}_3\text{N}_4$.⁴ According to these predictions, this phase could present insulating properties, hardness, and thermal conductivity comparable to those of diamond.

In nonstoichiometric $a\text{-CN}_x$ alloys the structural and electronic modifications introduced by N are not well understood. Moreover, mapping the valence band (VB) of $a\text{-CN}_x$ is important for further improvement of their optoelectronic properties. To our knowledge, few experimental papers have been devoted to studying the evolution of the top of VB on N content. Studies by photoelectron spectroscopy (PES) of the VB of $a\text{-CN}_x\text{:H}$ with N concentration up to 10% were reported by Mansour and Ugolini.⁵ The favorable effects of H in amorphous materials is well established.⁶ However, since H is not directly shown by PES the analysis of the photoemission spectra is troublesome. Even more important, perhaps, is the experimental evidence that H interrupts the connectivity of the C-N network.⁷ A different approach was followed by Mansour and Oelhafen.⁸ These authors studied the electronic structure of implanted graphite at room temperature with different N doses without annealing treatment. However, as the stress and defects caused by the implanted atoms distort the electronic structure we believe that these results are not quite general.

In this paper we present a comprehensive theoretical simulation and experimental determination of the density of states (DOS) of $a\text{-CN}_x$ alloys. The theoretical models assume C structures having different N content. These results are compared with the experimental spectra obtained by

PES. The aim of this work is twofold: (i) to study the influence of N on the VB (up to ~ 30 eV) and (ii) to elucidate the atomic local structure of $a\text{-CN}_x$ alloys containing N up to $x \sim 43\%$. To avoid the complications introduced by the presence of H, we have studied a set of nonhydrogenated $a\text{-CN}_x$.

II. EXPERIMENTAL PROCEDURE

The films were prepared *ex situ* by reactive radio-frequency sputtering of high purity graphite in a controlled atmosphere of Ar and N_2 gaseous mixture. The details of the material deposition are reported elsewhere.⁷ The x-ray excitation source was the Al $K\alpha$ photon (1486.6 eV, width 0.85 eV). The maximum N/C=43% ratio was obtained for the films grown in a 100% nitrogen atmosphere sputtering plasma. The VB spectra were measured using the He II line ($h\nu=40.8$ eV) from a He resonant lamp. The total system resolution was ~ 0.3 eV. As is well known, in amorphous materials the absence of long-range order implies the breakdown of the momentum conservation in an electronic transition. Therefore, the PES spectrum represents essentially the sum of the partial electronic DOS weighted by the electron photoionization cross section.⁹

III. THEORETICAL PROCEDURE

A. Core-level binding energy

The theoretical approach relies on calculations of DOS and core-level binding energies of model molecules containing C and N atoms. The calculations involved a combination of techniques that are described below, and the results are compared with the experimental spectra. Small molecules that are representative of the chemical bond in C-N alloys are chosen for evaluation of the chemical shifts on the N $1s$ electron binding energy. Figure 1 shows some of these structures that include sp , sp^2 , and sp^3 carbon hybridization and fragments of the theoretically predicted α and β carbon-nitride (C_3N_4) compound.^{4,10} Molecular conformations have been optimized within the Austin Model 1 (AM1) semiempirical technique.¹¹ Molecules representing C_3N_4 were taken from the predicted crystal structure and their confor-

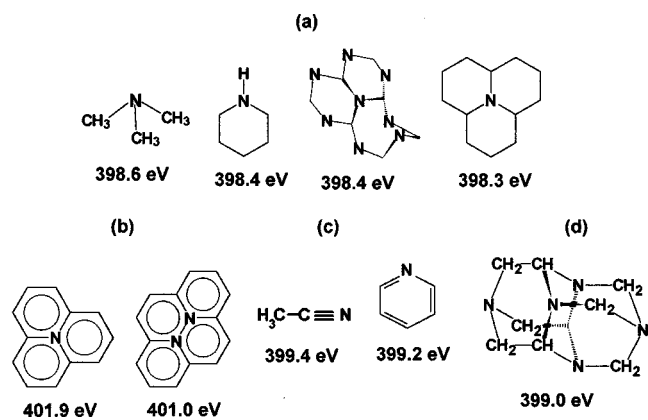


FIG. 1. Molecular structures considered and the resulting *ab initio* values of the N 1s core-level binding energies: (a) sp^3 N bonded to sp^3 C in open and closed structures; (b) sp^2 N substituting sp^2 C in aromatic structures; (c) sp N in a cyano compound and sp^2 N in pyridine; (d) sp^3 N bonded to sp^3 C in a closed structure in which C-N-C bond angles are stressed.

mations have not been optimized. The electronic structure was obtained by an *ab initio* 6-31*G calculation. Koopmans' theorem (KT) was used as an approximation to the N 1s binding energy.¹² As KT approximation does not account for electronic relaxation due to ionization phenomena, these values must be corrected. Recently, Casanovas *et al.*¹³ published *ab initio* calculations of core-level binding energy for N compounds explicitly considering electronic relaxation. Therefore, by comparison with these results, a scaling factor was obtained to correct the KT ionization energies. The numerical values associated to each structure are shown in Fig. 1. These calculations distinguish among four typical values of binding energies: (a) ~ 398.3 – 398.6 eV for threefold-coordinated N bonded to fourfold-coordinated sp^3 C; (b) ~ 401.9 – 401.0 eV for substitutional sp^2 N in graphitelike structures; (c) ~ 399.2 eV for sp^2 N (pyridinelike) or ~ 399.4 eV for sp N; and (d) ~ 399.0 eV for a stressed structure sp^3 N.

The comparison between our calculated N 1s electron binding energies for several chemical structures and some of the available experimental binding energies¹⁴ are in excellent

TABLE I. N 1s binding energies from *ab initio* calculations compared to experimental results.

	399.2	398.9, 399.3, 399.8 ^a
	400.1	400.4 ^a
	399.4	399.2 ^a
	398.5	398.5 ^a
H ₃ C-CN	399.4	399.4, 400.1 ^a
N ₂	402.5	403.0 ^b
	398.9	398.6 ^a
H ₃ C-N=CH ₂	399.0	--

^a Reference 14(a).

^b Reference 14(b).

agreement, as shown in Table I, giving us the confidence to look for trends explaining our results.

The formation of paracyanogenlike compounds was recently theoretically suggested.¹⁵ Therefore, for comparison purposes, a paracyanogenlike compound has been specifically included in the table. We notice that the N 1s electron binding energy obtained in this compound lies in the 399.0-eV region, which is not observed in the experimental x-ray photoemission spectroscopy (XPS) spectrum. Moreover, we would like to point out that synthesized paracyanogen, a compound having an extended π structure within fused carbon rings, shows the N 1s electron binding energy at ~ 403 eV, far away from the binding energies found in CN_x materials.¹⁶

B. Valence-band electronic structure

Large clusters including up to 54 carbon atoms in the graphite symmetry structure were adopted to study the VB electronic structure through substitution of C with N atoms. All dangling bonds at the boundaries were saturated with H atoms. Substitutional N atoms randomly distributed in graphite clusters for concentrations N/C of 12%, 17%, and 29% were considered. Molecular conformations have been optimized within the AM1 technique. Clusters formed by C tetrahedrally bonded to N are taken from the predicted crystal structures of α and β polytype phases of C₃N₄ without geometry optimization, and typically included 36 C and 48 N atoms.¹⁰ The electronic structure was obtained by the valence effective Hamiltonian (VEH) method.¹⁷ This is a pseudopotential technique giving one-electron spectra of *ab initio* double-zeta quality and it was successfully applied to organic materials. The same scaling factor found for N core levels was applied to the valence levels since both calculations are of comparable level of accuracy. For comparison purposes, the Fermi energy of the pure graphite cluster was shifted to zero. Histograms were obtained by the usual counting of states procedure. The DOS were then simulated by a convolution of the histograms with Gaussian line shapes with an arbitrary broadening of 0.5 eV. It is usual in the above procedure to obtain simulated spectra showing some small oscillations due to finite-size effects. The simulated DOS for the pure graphite cluster reproduces very well the experimental spectra reported in the literature and the spectra obtained for *a*-C films prepared in our deposition chamber. We did not find any qualitative difference in the DOS for α and β phases of C₃N₄, hence all further discussions will be based upon the result for the β phase. The above described calculations have been performed in SPARTAN package¹⁸ and Cerius², a program developed by Molecular Simulations Inc.

IV. DISCUSSION

Figure 2 shows the experimental evolution of the N 1s core-level spectra on N concentration. The inelastic background was subtracted using Shirley's method.¹⁹ The curves show two well-resolved structures at 398.2 and 400.5 eV (from now on peaks P_1 and P_2) associated with N atoms in two quite different local configurations.⁷ Peak P_1 becomes dominant in the material containing high N concentration. This suggests that, depending on the amount of N incorpo-

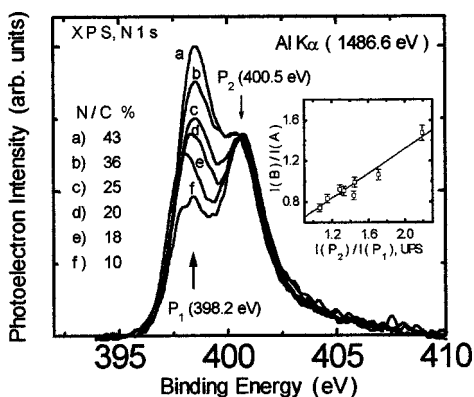


FIG. 2. Photoemission spectra of the N $1s$ core level of the a -CN $_x$ alloy. Inset: Ratio $I(A)/I(B)$ vs $I(P_2)/I(P_1)$, where I stands for the photoemission intensity. The symbols in parentheses identify either the structure in the XPS or UPS spectra (Figs. 2 and 3).

rated in the sample, a particular structure is favored (curve a , Fig. 2). The *ab initio* simulation shows that the N $1s$ spectra of configurations containing N bonded to C sp^3 and substitutional N sp^2 are consistently near to the position of peaks P_1 and P_2 , respectively. These conclusions are indeed similar to the ones drawn by Marton, Boyd, and Rabalais²⁰ that interpreted peaks P_1 and P_2 as evidence of the existence of two well-defined phases in the material. Finally, in agreement with Sjöström *et al.*,²¹ the experimental evidence that P_1 becomes dominant for large N content suggests that the N coordination goes from a planar structure to a three-dimensional structure.

Figure 3(a) shows the ultraviolet photoemission spectroscopy (UPS) spectra of the studied samples. The Fermi level E_F is arbitrarily located at $E=0$. Spectra of a -CN $_x$:H ($0 < x < 0.1$) were measured *in situ* by Mansour and Ugolini.⁵ These spectra compare very well with the spectra obtained in this work when samples containing an equal amount of N are considered. The spectrum of pure a -C [Fig. 3(a)] shows two bands located at binding energies ~ 7.7 and ~ 3.6 eV, respectively. As shown by other investigators, these bands are σ and π bonds due to C $2p$ electrons.¹ On increasing N content three new features emerge at energies near to ~ 9.5 , ~ 7.1 , and ~ 4 – 5 eV. For N/C ratios larger than 20%, the bands at 7.7 and 3.6 eV present in pure carbon disappear completely. Also, the band at 7.1 eV dominates the spectrum for films with intermediate N content ($10\% < N/C < 25\%$). The bands at ~ 9.5 and ~ 4 – 5 eV are wider and increase slowly for larger N/C ratios ($> 25\%$). These bands dominate the spectra for the highest nitrogenated samples. Finally, the leading edge of the VB recedes on increasing N content.

The simulated DOS for N-substituted graphite clusters are displayed in Fig. 3(b). Curve a in this figure corresponds to the pure graphite cluster. It presents two well-defined structures at binding energies of ~ 4 and ~ 8 eV, associated to π and σ bonds, respectively. As N is progressively incorporated in the cluster, these two bands are pushed to higher binding energies, as observed in curves b – d of Fig. 3(b). At the highest N concentration considered ($N/C=29\%$), the band associated with π bonds has shifted to ~ 7.1 eV while the one associated with σ bonds has broadened and shifted to ~ 11 eV. A new feature appears close to the Fermi energy

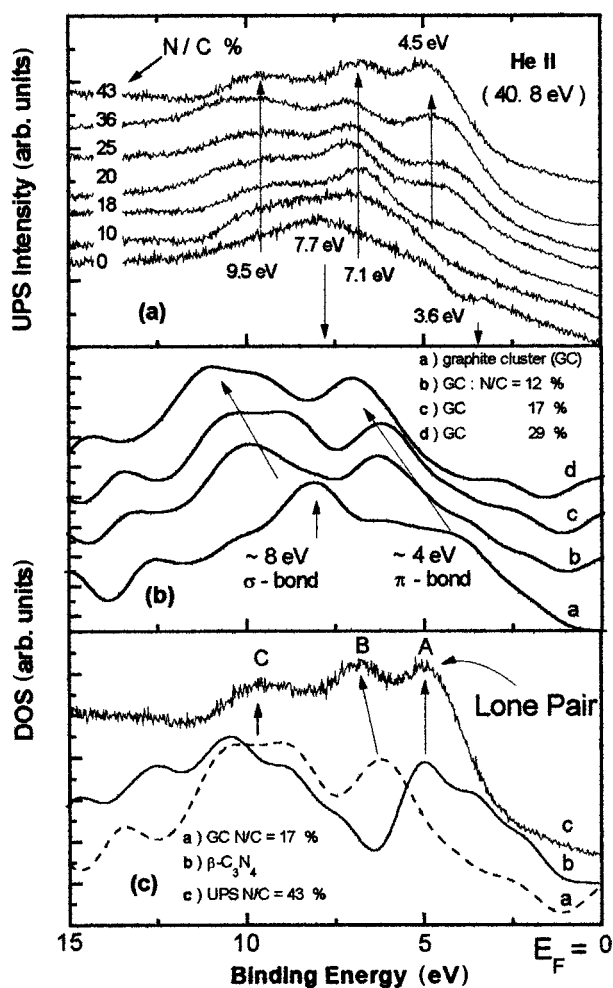


FIG. 3. Valence-band photoelectron spectra and simulated densities of states of carbon nitride. (a) He II UPS intensities (arbitrary units) as a function of binding energies (eV) for $0 \leq N/C \leq 0.43\%$ ratio. Upward (downward) arrows denote features that increase (decrease) on increasing N content. The average peak energy is indicated. (b) Simulated densities of states for graphite (curve a) and randomly N-substituted graphite clusters (curves b – d) having N/C concentrations of 12–29%. (c) Simulated DOS for (curve a) N-substituted graphite cluster with N/C=17%, (curve b) β -C $_3$ N $_4$ cluster, and (curve c) experimental UPS spectra for the sample with N/C=43%. Peaks A, B, and C are assigned to N lone pairs of the β -C $_3$ N $_4$ structure, C-N π bonds of substitutional N in graphite structures, and C-N σ bonds, respectively.

due to the fact that sp^2 N in a planar graphite structure contribute with two electrons to the π system. This is probably the reason for the system to change into a three-dimensional full sp^3 structure in which the N π electrons turn into nonbonding lone pairs.

Aside from oscillations that are due to the finite cluster size, the calculated DOS for the β -C $_3$ N $_4$ structure [Fig. 3(c), curve b] presents two bands located at ~ 5 and ~ 10 eV. The former is related to N lone-pair electrons while the latter is akin to σ orbital of C-N bonds. The structure in the 0–5 eV binding-energy region corresponds to N lone-pair electrons localized at the cluster boundaries. Therefore, they are expected to move toward the peak located at 5 eV on increasing cluster size. For comparison purposes the calculated DOS of the graphitelike cluster for N/C=17% ratio is also

shown in curve *a*, Fig. 3(c). In this curve the absence of the structure located at ~ 5 eV associated to N lone-pair electrons is apparent. The present simulation allows us to identify three regions: (1) a band located at ~ 5 eV that is associated to N lone pairs; i.e., N and C are assumed to form a structure similar to crystalline silicon-nitride where C is sp^3 hybridized; (2) a band located at ~ 7.1 eV associated with electrons occupying π orbitals of C-N bonds; (3) a band located at ~ 9.5 – 11 eV associated to σ orbitals of C-N bonds.

Next we proceed with the analysis of the experimental spectra in relation to the simulation results. For the sake of clarity we plotted in Fig. 3(c) only the He II spectrum of the highest nitrogenated sample (N/C \sim 43% ratio). A comparison of the experimental curve with the theoretical simulations suggests that peaks *A*, *B*, and *C* are due to N lone-pair electrons, π electrons of C-N bonds, and σ electrons of C-N bonds, respectively. Moreover, in order to reproduce the total DOS of samples with N/C $>$ 20% ratio, it is necessary to assume a partial contribution of DOS due to N lone-pair electrons as in the β -C₃N₄ phase (see Fig. 3). Below N/C \sim 18–20 % ratio, the lack of structure at ~ 4 – 5 eV in the experimental curves suggests that N is occupying sites in graphitelike structures.

In a recent theoretical article by Weich, Widany, and Frauenheim,¹⁵ the valence band of *a*-CN_x (57% N) was calculated. This calculation shows only two peaks located at ~ 2.5 and ~ 7.0 eV below the Fermi energy, respectively. Clearly, these results do not account for the actual experimentally observed three peaks located at 4–5, 7.1, and 9.5 eV, respectively [Fig. 3(a)].

As discussed above, P_1 was associated to threefold-coordinated N bonded to sp^3 C fourfold coordinated. On the other hand, P_2 was associated to substitutional N sp^2 . Therefore, it is expected that P_1 and P_2 will be related to the structure associated with N lone-pair electrons (peak *A*) and to π electrons (peak *B*), respectively [Fig. 3(c)]. In order to test this hypothesis, we plotted the ratio $I(A)/I(B)$ versus $I(P_2)/I(P_1)$ (Fig. 2, inset). Here, *I* stands for intensity and the symbols in parentheses identify either the structure in the UPS or in the core-level spectra. The quite good linear correlation in Fig. 2 (inset) confirms our assumption. Therefore, one can conclude that below the N/C \sim 18–20 % ratio, N is occupying a C site in graphitelike structures. Above N/C \sim 18–20 % ratio, the alloy tends to form a three-

dimensional structure with C and N atoms fourfold and threefold coordinated, respectively, possibly as the predicted β -C₃N₄ phase.

V. CONCLUSIONS

In summary, the electronic structure of sputtered *a*-CN_x films was experimentally determined by photoemission electron spectroscopy. The valence-band DOS and core-level binding energies were numerically determined by model molecules containing C and N atoms. The incorporation of N produces N 1s spectra with two peaks that are correlated to the evolution of the top of the valence band. The numerical simulation of core-level energies suggests that the peak at the lower binding energy (398.2 eV) is due to N atoms in a configuration with isolated lone pairs, as in β -Si₃N₄. The peak located at the higher binding energy (400.5 eV) is attributed to substitutional N atoms in a sp^2 graphitelike configuration. In this case, the lone-pair electrons are not isolated, i.e., they are involved in stronger π bonds of aromatic rings.

In conclusion, for increasing N content three new bands (called *A*, *B*, and *C*) dominate the top of the VB. The following interpretation stems from the numerical simulation: (i) the band *A*, located at ~ 4.5 eV, is due to lone-pair electrons belonging to N atoms; (ii) the band *B*, located at ~ 7.1 eV, is due to C 2*p* and N 2*p* electrons associated to π bonds in aromatic rings containing at least one substitutional N atom; (iii) the band *C*, located at ~ 9.5 eV is also due to C 2*p* and N 2*p* electrons but shared in σ bonds.

Finally, we stress two points: (1) in order to reproduce the total density of states in samples with the N/C ratio larger than 20%, it was necessary to assume a partial contribution due to lone-pair electrons as in the β -C₃N₄ phase; and (2) below N/C \sim 20% the material has predominantly a graphitelike structure.

ACKNOWLEDGMENTS

The authors are indebted to A. Zanatta for a critical reading of the manuscript. M.C.S. acknowledges Professor J. L. Brédas for the valence effective Hamiltonian package. This work was partially sponsored by Fundação de Amparo a Pesquisa Do Estado De São Paulo (Grant Nos. 91/3635-6 and 94/3639-0), Programa de Apoio ao Desenvolvimento da Ciencia e Tecnologia, and European Commission (CI1*-CT93-0062). The authors acknowledge financial support from CNPq.

¹J. Robertson, Philos. Trans. R. Soc. London, Ser. A **342**, 277 (1993), and references therein.

²D. F. Franceschini, C. A. Achete, and F. L. Freire, Jr., Appl. Phys. Lett. **60**, 3229 (1992).

³D. I. Jones and A. D. Stewart, Philos. Mag. A **46**, 423 (1982); H. X. Han and B. J. Feldman, Solid State Commun. **65**, 921 (1988).

⁴A. Liu and L. Cohen, Science **245**, 841 (1989).

⁵A. Mansour and D. Ugolini, Phys. Rev. B **47**, 10 201 (1993).

⁶R. A. Street, *Hydrogenated Amorphous Silicon* (Cambridge University Press, New York, 1991).

⁷S. Souto and F. Alvarez, Appl. Phys. Lett. **70**, 1539 (1997).

⁸A. Mansour and P. Oelhafen, Appl. Phys. A: Solids Surf. **58**, 437 (1994).

⁹P. Oelhafen, in *Amorphous and Liquid Material*, NATO Advanced Study Institute, Series E: Applied Sciences, Vol. 118, edited by E. Luscher, G. Fritsch, and G. Jacucci (Martinus Nijhoff, Dordrecht, 1987).

¹⁰Y. Guo and W. A. Goddard III, Chem. Phys. Lett. **237**, 72 (1995).

¹¹M. J. S. Dewar, E. G. Zoebish, E. F. Healy, and J. J. P. Stewart, J. Am. Chem. Soc. **107**, 3902 (1985).

¹²T. Koopmans, Physica (Amsterdam) **1**, 104 (1934).

¹³J. Casanovas, J. M. Ricart, J. Rubio, F. Illas, and J. M. Jiménez-

- Mateos, J. Am. Chem. Soc. **118**, 8071 (1996).
- ¹⁴(a) NIST X-ray Photoelectron Spectroscopy Database Version 2.0, National Institute of Standards and Technology (Gaithersburg, MD, 1997); (b) *Practical Handbook of Spectroscopy*, edited by J. W. Robinson (CRC, Boca Raton, FL, 1991).
- ¹⁵F. Weich, J. Widany, and Th. Frauenhein, Phys. Rev. Lett. **78**, 3326 (1997).
- ¹⁶L. W. Jenneskens, J. W. G. Mahy, E. J. Vliestra, S. J. Goede, and F. Bickelhaupt, J. Chem. Soc. Faraday Trans. **90**, 327 (1994).
- ¹⁷R. Lazzaroni, N. Sato, W. R. Salaneck, M. C. dos Santos, J. L. Brédas, B. Tooze, and D. T. Clark, Chem. Phys. Lett. **175**, 175 (1990), and references therein.
- ¹⁸SPARTAN, Wavefunction Inc., Irvine, CA, 1995.
- ¹⁹D. A. Shirley, Phys. Rev. B **5**, 4709 (1972).
- ²⁰D. Marton, K. J. Boyd, and J. W. Rabalais, Int. J. Mod. Phys. B **9**, 3527 (1995).
- ²¹H. Sjöström, S. Stafström, M. Boman, and J.-E. Sundgren, Phys. Rev. Lett. **75**, 1336 (1995).